Influence of electronic energy deposition on the structural modification of swift heavy-ion-irradiated amorphous germanium layers

T. Steinbach,[1,*] C. S. Schnohr,[1] P. Kluth,[2] R. Giulian,[2] L. L. Araujo,[2] D. J. Sprouster,[2] M. C. Ridgway,[2] and W. Wesch[1]

[1]*Institut für Festkörperphysik, Friedrich-Schiller-Universität Jena, Max-Wien-Platz 1, D-07743 Jena, Germany*

[2]*Australian National University, Research School of Physics and Engineering, Canberra ACT 0200, Australia*

(Received 7 June 2010; revised manuscript received 20 October 2010; published 24 February 2011)

Swift heavy-ion (SHI) irradiation of amorphous germanium (a-Ge) layers leads to a strong volume expansion accompanied by a nonsaturating irreversible plastic deformation (ion hammering), which are consequences of the high local electronic energy deposition within the region of the a-Ge layer. We present a detailed study of the influence of SHI irradiation parameters on the effect of plastic deformation and structural modification. Specially prepared a-Ge layers were irradiated using two SHI energies and different angles of incidence, thus resulting in a variation of the electronic energy deposition per depth ϵ_e between 14.0 and 38.6 keV nm^{-1}. For all irradiation parameters used a strong swelling of the irradiated material was observed, which is caused by the formation and growth of randomly distributed voids, leading to a gradual transformation of the amorphous layer into a sponge-like porous structure as established by cross-section scanning electron microscopy investigations. The swelling depends linearly on the ion fluence and on the value of ϵ_e, thus clearly demonstrating that the structural changes are determined solely by the electronic energy deposited within the amorphous layer. Plastic deformation shows a superlinear dependence on the ion fluence due to the simultaneous volume expansion. This influence of structural modification on plastic deformation is described by a simple approach, thus allowing estimation of the deformation yield. With these results the threshold values of the electronic energy deposition for the onset of both structural modification and plastic deformation due to SHI irradiation are determined. Furthermore, based on these results, the longstanding question concerning the reason for the structural modification observed in SHI-irradiated crystalline Ge is answered.

DOI: 10.1103/PhysRevB.83.054113 PACS number(s): 61.80.Jh, 61.43.Dq, 62.20.F−, 61.43.Gt

I. INTRODUCTION

Ion-irradiation-induced structural modifications in amorphous germanium (a-Ge) were first reported following low-energy heavy-ion irradiation (several hundred kilo–electron volts).[1–8] In this energy range the ions are stopped mainly by elastic scattering with the target atoms. This process, referred to as nuclear energy deposition ϵ_n, typically has values of a few kilo–electron volts per nanometer and results in the displacement of target atoms. Wilson[1] showed that after the crystalline-to-amorphous transformation at an ion fluence of $N_I \approx 10^{14}$ ions cm^{-2}, formation of surface voids as well as surface craters occurred at $N_I \approx 10^{15}$ ions cm^{-2} in a-Ge. Further investigations revealed a morphological instability of the amorphous phase[5,6,8] for ion fluences $N_I > 10^{16}$ ions cm^{-2}, leading to the formation of nanovoids within the amorphous material.[8] With increasing fluence, this finally resulted in the formation of a stable porous sponge-like structure accompanied by dramatic swelling of the irradiated material.

For high-energy heavy-ion irradiation (energy above 100 MeV), a similar volume expansion can be observed.[9–11] Here, the dominant stopping process is the inelastic interaction of ions with target atoms, known as electronic energy deposition ϵ_e, with values of ≈10–60 keV nm^{-1}. Within less than 10^{-16} s this process induces a high density of electronic excitations and ionizations along the ion path, the latter having a length of several micrometers, and the radial extension of the excited track has a diameter of a few nanometers. The high electronic energy density leads to atomic motion potentially caused by a Coulomb explosion,[12–14] nonthermal melting,[15–19] and/or electron-phonon coupling.[20–22] As a consequence, a volume-conserving plastic deformation[23–28] and the formation of amorphous tracks[29–31] can be observed for many amorphous and crystalline materials, respectively, for high values of ϵ_e. In the case of crystalline germanium (c-Ge), tracks have not been observed after single-ion irradiation with 600 MeV Au ions ($\epsilon_e = 35$ keV nm^{-1}).[32] However, discontinuous tracks (pearl-like distributions of amorphous clusters along the ion trajectory) have been registered after SHI irradiation with 710 MeV Bi, which corresponds to an electronic energy deposition above 37 keV nm^{-1}.[33] It was shown that swift heavy-ion (SHI) irradiation of c-Ge also yielded a significant volume expansion over the irradiated area,[9] due to the formation of a buried porous sponge-like layer after irradiation with high-energy Au ions. However, the porous structure was formed at approximately two-thirds the depth of the nuclear energy deposition maximum, and thus it may depend on both electronic and nuclear energy deposition. Recently, nonperpendicular SHI irradiation of a-Ge surface layers at room temperature has been studied for the first time.[10] A plastic flow process in the direction of the ion beam projection on the sample surface accompanied by extreme swelling of the irradiated areas was observed. This swelling of the a-Ge surface layer during SHI irradiation is caused by the transformation to a sponge-like structure similar to that observed for low-energy ion irradiation. However, in this case the structural modification was solely due to the high electronic energy deposition. As a consequence of the change in morphology, a nonlinear plastic flow, that is, an *enhanced* plastic flow, occurred. Nevertheless, it was concluded from this investigation that a-Ge flows plastically in the same way as amorphous silicon (a-Si)[34–36] and conventional glasses[23,25,37] during nonperpendicular ion irradiation. Moreover, the results

in Ref. 10 show evidence of neither recrystallization of the amorphous layer nor track formation in a-Ge due to the high electronic energy deposition, which is in contradiction to the results reported in Refs. 38 and 39, respectively. There the observed tracks in thin evaporated Ge films with track diameters of 8 to 23 nm ($\epsilon_e \geqslant 5.3$ keV nm^{-1}) consist of small crystallites or recrystallized regions, which are assumed to be a consequence of local melting (thermal spike).[39] However, calculations in the framework of the extended thermal spike model revealed a maximum lattice temperature of ≈580 K for 200 MeV Au ion irradiation in c-Ge ($\epsilon_e \approx 25$ keV nm^{-1}).[40] This temperature is half that required for melting. However, it must be mentioned that, compared to crystalline materials, higher temperatures could be achieved in amorphous materials due to the atomic disorder. Thus, in amorphous materials the electron-phonon coupling constant is higher and therefore the energy deposition is more localized in amorphous solids.[41] Thus track formation could occur at lower energy deposition in amorphous materials than in crystalline ones. The nucleation of a crystalline phase induced in the quenched-in liquid phase after SHI irradiation (observed in Ref. 41) may be attributed to the lower phonon mean free path and lattice thermal conductivity in this amorphous material. Consequently, we speculate that the initial structure of the 5 nm-thick Ge films about which no information was given and the *thin* film itself, in combination with the *large* incident angle of 80°, plays an important role for the different effect observed in Ref. 39.

The purpose of the present paper is to investigate the formation of voids within the amorphous surface layer as functions of the ion energy and angle of incidence, that is, varying electronic energy deposition, in detail. For all irradiation conditions, swelling of the irradiated areas can be observed, which depends linearly on the ion fluence. Moreover, the rate of swelling depends on the electronic energy deposition ϵ_e. This enables the estimation of an electronic energy deposition threshold, above which the swelling, that is, void formation, begins. The influence of swelling on the plastic flow process can be described by a simple approach, which provides an opportunity to derive the deformation yield for the given irradiation parameters. This enables an estimation of the electronic energy deposition threshold for the ion hammering effect in a-Ge in an analogous manner to a-Si.[34]

II. EXPERIMENTAL PROCEDURE

Homogeneous a-Ge layers were produced by multiple Ge ion implantations into 500 μm-thick (100) Ge substrates at 80 K using various ion energies between 0.08 and 6.70 MeV and ion fluences in the range of 0.49 to 2.73 × 10^{14} cm^{-2}. Rutherford backscattering spectrometry in a channeling configuration and cross-section transmission electron microscopy (TEM) studies of the implanted samples confirmed an amorphous surface layer free of voids and cavities, with a thickness of 3.1 μm. To investigate the effect of SHI irradiation on structural modification and plastic flow, a gold (Au) grid of approximately 40 nm thickness was deposited on the sample surface.

SHI irradiation was performed at room temperature using 89 MeV Au^{9+} and 185 MeV Au^{13+} ions. The angle of incidence Θ varied between 0°, 45°, and 60° relative to the surface normal. Due to the high ion energies the nuclear energy deposition was negligible and the electronic energy deposition dominated the energy transfer at the surface, varying between 14.0 and 38.6 keV nm^{-1} (see Table I), as estimated by SRIM 2008 calculations.[42] Note that the electronic energy deposition decreased slightly over the depth of the a-Ge layer, and hence an average value of ϵ_e was taken for the whole layer. At a constant ion flux of 2 × 10^{10} cm^{-2} s^{-1}, the fluences, which refer to the number of ions per square centimeter (projection of the beam cross section on the surface), ranged between 1.0 × 10^{12} and 1.5 × 10^{14} cm^{-2}. Under these irradiation conditions the Au ion range is significantly greater than the extent of the amorphized surface layer. Details of the SHI irradiation conditions are listed in Table I.

TABLE I. Conditions of swift heavy gold irradiation, where Θ, R_p, ϵ_e, and N_I denote the angle of incidence with respect to the surface normal, the projected range of Au ions, the electronic energy deposition calculated with SRIM 2008,[42] and the ion fluence range, respectively. Irradiation was performed at room temperature with an ion flux of 2 × 10^{10} cm^{-2} s^{-1}.

E (MeV)	Ion	Θ (deg)	R_p (μm)	ϵ_e (keV nm^{-1})	N_I (cm^{-2})
89	Au^{9+}	0	10.5	14.0	4.5 × 10^{13}
		45	7.5	18.1	1.0 × 10^{12} to 1.5 × 10^{14}
185	Au^{13+}	0	15.7	21.0	1.0 × 10^{12} to 1.5 × 10^{14}
		45	11.0	28.3	1.0 × 10^{12} to 1.5 × 10^{14}
		60	8.0	38.6	1.0 × 10^{12} to 1.5 × 10^{14}

To quantify the swelling and the plastic flow, one-half of the sample was masked with an aperture inhibiting ion penetration to enable the comparison of irradiated and unirradiated material. Samples were analyzed *ex situ* after irradiation by means of surface profilometry, optical microscopy and scanning electron microscopy (SEM), which was used in plan-view as well as two different cross-section geometries (XSEM).

III. EXPERIMENTAL RESULTS

Figure 1 shows as an example an optical micrograph of the surface of the a-Ge layer with the Au marker layer. The lower part of the sample was irradiated under a nonperpendicular ion incidence (Θ = 45°, from the right side; Fig. 1) with 89 MeV Au ions to an ion fluence of 1.5 × 10^{14} cm^{-2}, whereas the upper part of the sample was masked (unirradiated).

In Fig. 1 the two effects, namely, plastic deformation and swelling, are both obvious. The Au squares spanning the irradiated/unirradiated boundary on the sample surface demonstrate the positive shift of the irradiated area, that is, during nonperpendicular SHI irradiation, a-Ge flows plastically in the direction of the ion beam projection on the sample surface (see arrows in Fig. 1).

Compared to the masked unirradiated upper half of the sample, the reflectivity of the Ge surface (lines between gold squares) is reduced for all irradiation parameters with increasing ion fluence. The higher magnification SEM figure in the inset shows a section close to the irradiated/unirradiated

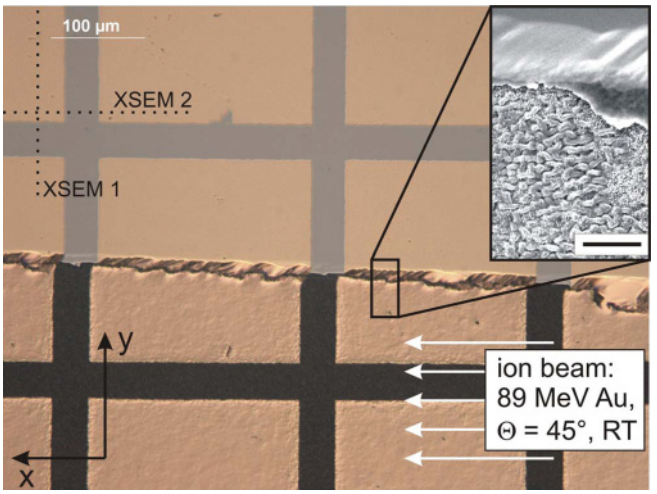

FIG. 1. (Color online) Optical micrograph showing the swelling as well as the plastic flow of the irradiated amorphous germanium layer during SHI irradiation with 89 MeV Au ions under an angle of $\Theta = 45^\circ$ from the right with the ion fluence $N_I = 1.5 \times 10^{14}$ cm^{-2} at room temperature. Inset: SEM image at a higher magnification of the same sample close to the swelling edge (scale bar: 5 μm). In addition, the two breaking edges for XSEM are indicated schematically by dotted lines.

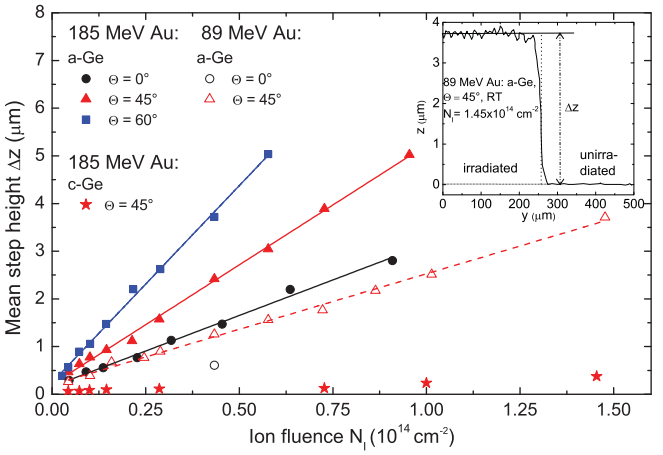

FIG. 2. (Color online) Mean step height Δz of the surface for amorphous germanium layers (a-Ge) irradiated with different ion energies and different angles of incidence Θ as a function of the ion fluence. Also shown are data for crystalline germanium (c-Ge) irradiated with 185 MeV Au under 45° as a reference sample. Data were fitted linearly (solid and dashed lines). Inset: swelling of an irradiated a-Ge layer as measured by the surface profilometer.

boundary, where the Au marker layer on the irradiated area was partly removed. Compared to the unirradiated Ge surface, which is planar with very low surface roughness, the irradiated Ge parts exhibit considerably increased surface roughness.

A. Formation of voids: Swelling

For Au ion irradiation with different ion energies and different angles of incidence (cp. Table I) a significant expansion of the irradiated a-Ge layer relative to the unirradiated part was observed (cf. Fig. 1). This swelling is shown as a function of the implantation parameters in Fig. 2, where the mean value of the step height Δz is depicted as a function of the ion fluence. As an example, the inset shows the swelling of an irradiated a-Ge layer as measured by the surface profilometer for 89 MeV Au irradiation to an ion fluence of 1.45×10^{14} cm^{-2}. The swelling of the irradiated part is clearly evident. Besides this volume expansion, a significant increase of the surface roughness of the irradiated area was also observed. Accordingly, the step height values shown in Fig. 2 represent an average value obtained from 5 to 10 separate measurements.

The step height of the irradiated a-Ge layer increases with increasing ion fluence for all irradiation parameters and exhibits a linear dependence on the ion fluence,

$$\Delta z = \alpha N_I, \tag{1}$$

with a fit parameter α. In Table II these slopes α as well as the step heights Δz for a fixed ion fluence of 4.5×10^{13} cm^{-2} are summarized for all ion energies and angles of incidence used for irradiation. Considering the step height for an angle of incidence of 45°, the comparison between the two irradiation energies shows that the step height of the 89 MeV irradiation is approximately half the value of that measured for 185 MeV irradiation (see Fig. 2). This can be attributed to the lower ion energy and, consequently, to the lower electronic energy deposition over the a-Ge layer (see Table I). Furthermore, an increase in Δz is observed with increasing angle of incidence due to the increased electronic energy deposition (21.0, 28.3, and 38.6 keV nm^{-1} for an angle of incidence of 0°, 45°, and 60°, respectively). Hence, the maximum step height measured at the ion fluence of 4.5×10^{13} cm^{-2} amounts to approximately 4 μm (see Table II) for irradiation with 185 MeV Au and an incident angle of 60°. Note that for all irradiation parameters used, saturation of swelling was not observed for the given range of ion fluences.

In contrast to the amorphous samples, no significant swelling was observed for the crystalline reference sample irradiated with 185 MeV Au ions under a 45° ion incidence (see Fig. 2). The measured step heights are less than 100 nm up to an ion fluence of 1.0×10^{14} cm^{-2}. With further irradiation a slightly increased step height was found, which amounts to 350 nm for the highest ion fluence of 1.5×10^{14} cm^{-2} (see Sec. IV A). Furthermore, no change in reflectivity occurred, in contrast to the amorphous samples, suggesting that the origin of the swelling is not at the surface of the irradiated crystalline material.

TABLE II. Slope α, determined on the basis of Fig. 2, as well as the measured step height Δz for a fixed ion fluence of 4.5×10^{13} cm^{-2} are given for the swift heavy-ion irradiation with different ion energies (E) and different angles of incidence (Θ).

E (MeV)	Θ (deg)	α (10^{-14} μm cm^2)	Δz (μm)
89	0	–	0.61 ± 0.02
	45	2.33 ± 0.02	1.26 ± 0.02
185	0	2.98 ± 0.04	1.47 ± 0.03
	45	5.02 ± 0.04	2.45 ± 0.04
	60	8.26 ± 0.07	4.03 ± 0.05

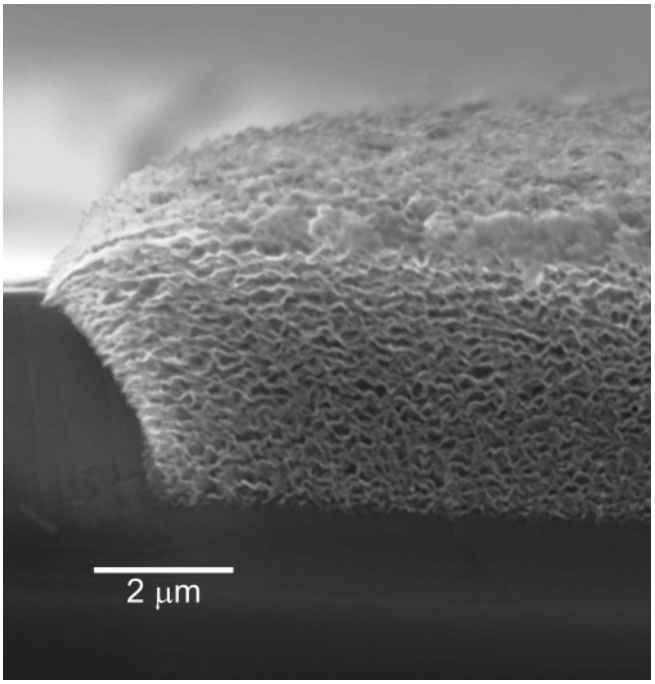

FIG. 3. XSEM image (XSEM 1; cf. Fig. 1) showing the transformation of the homogeneous amorphous germanium layer into a sponge-like porous germanium layer after irradiation with 89 MeV Au ions under an angle of $\Theta = 45^\circ$ with an ion fluence of 1.0×10^{14} cm^{-2}.

The a-Ge samples, for which a fluence dependence of the volume expansion was observed, were investigated after irradiation by XSEM. The image in Fig. 3 shows a cross section perpendicular to the projection of the ion beam (XSEM 1; cf. Fig. 1) and reveals the cause of the swelling. The transformation of the initially homogeneous a-Ge surface layer into a porous sponge-like layer is clearly visible. The formation of voids, which accumulate with increasing ion fluence to form a porous layer,[10] takes place solely in the 3.1 μm-thick amorphous surface layer; the underlying substrate is still crystalline and free of voids. The distinct porous/crystalline boundary is the original amorphous/crystalline boundary. The voids themselves are irregularly shaped, have sizes of several hundreds of nanometers, and are not aligned along a preferred orientation. A part of the sample that was masked during the irradiation is visible in the left part of the image in Fig. 3. There, no voids were generated.

B. Plastic deformation: Surface shift

After nonperpendicular SHI irradiation, a positive shift of the irradiated a-Ge layer with respect to the unirradiated part is clearly visible in Fig. 1. This surface shift Δx, determined on the basis of such images (e.g., Fig. 1, but with higher resolution and magnification), is shown in Fig. 4 as a function of the ion fluence for the irradiation parameters investigated. All curves show a nonlinear behavior (demonstrated by the linear function in Fig. 4; dashed black line), that is, the enhanced plastic flow process that was demonstrated recently.[10] The steep increase in the surface shift is thus correlated with the formation and growth of voids within the amorphous surface

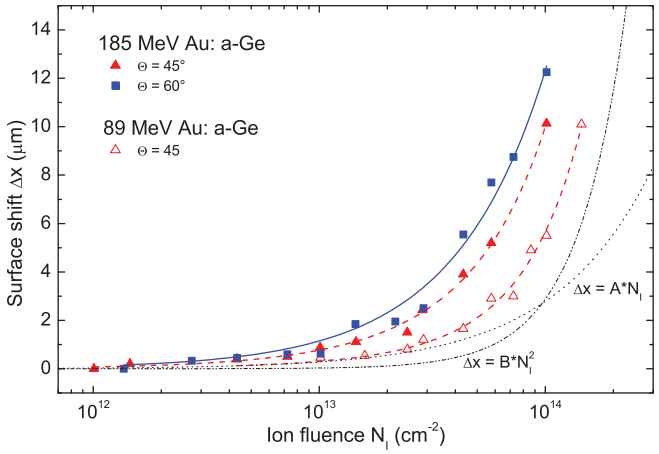

FIG. 4. (Color online) Surface shift Δx of the amorphous germanium layer as a function of the ion fluence for different nonperpendicular irradiation conditions. Lines (solid and dashed) are fits to the data using Eq. (3). For comparison, dotted and dash-dotted lines represent a linear and a quadratic function, respectively.

layer (see Fig. 2). Consequently, the density reduction causes the increased rate of surface shift with increasing ion fluence.

It is well known that the surface shift Δx depends on the incident angle Θ, $\Delta x \propto \sin(2\Theta)$, as well as on the electronic energy deposition ϵ_e [see Sec. IV B; Eq. (2)], and hence the curves are offset with respect to each other. The 89 MeV curve is shifted to higher ion fluences compared to both 185 MeV irradiations, due to the significantly lower electronic energy deposition (cf. Table I). The slight shift observed for the 185 MeV irradiations themselves is a result of the directly opposed influence [see Eq. (2)] of the electronic energy deposition, with a ratio of $\epsilon_e^{60^\circ}/\epsilon_e^{45^\circ} = 1.4$, and the angle of incidence, with a ratio of $\sin(2 \times 60^\circ)/\sin(2 \times 45^\circ) = 0.86$.

In accordance with previous investigations,[10,34–36] no plastic flow, that is, no surface shift, was observed for the a-Ge layer during perpendicular ion incidence or for the crystalline sample under both perpendicular and nonperpendicular irradiation.

In Fig. 5 an XSEM image of the same sample shown in Fig. 3 is depicted. However, here the cross section was taken parallel to the projection of the ion beam (XSEM 2; cf. Fig. 1). The sample was irradiated with 89 MeV from the right-hand side with an angle of incidence of $\Theta = 45^\circ$. Due to this cross-section geometry it becomes apparent that the voids are orientated within the a-Ge layer. However, their orientation does not appear to correspond to the direction of the ion tracks along which the energy is deposited into the electronic system of the a-Ge layer but, rather, reflects the ion-beam-induced plastic flow process in the positive direction directly.

IV. DISCUSSION

A. Formation of voids: Swelling

Concerning the step height measurements in Fig. 2, the influence of the electronic energy deposition on void formation within the a-Ge layer is clear. In Fig. 6 the slopes determined from Fig. 2 (and listed in Table II) are depicted as a function

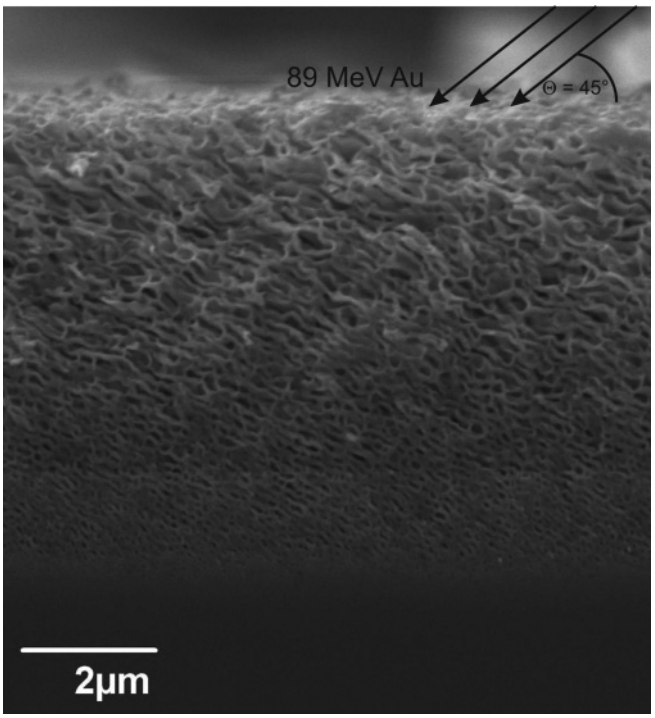

FIG. 5. XSEM image showing a cross section parallel to the projection of the ion beam (XSEM 2; cf. Fig. 1), after an irradiation with 89 MeV Au ions under an angle of $\Theta = 45^\circ$ (from the right) with an ion fluence of 1.0×10^{14} cm^{-2}. The ion-beam-induced plastic flow process is directly reflected by the void orientation.

of the electronic energy deposition ϵ_e. The slope increases linearly with increasing energy deposition. The extrapolation of the regression line yields an electronic energy deposition of about $\epsilon_e = 10.5 \pm 1.0$ keV nm^{-1} for a zero step height. This means that for room-temperature irradiation, a threshold value of the electronic energy deposition can be determined above which the swelling, that is, the formation of voids, begins. The existence of this threshold value of 10.5 ± 1.0 keV nm^{-1} is

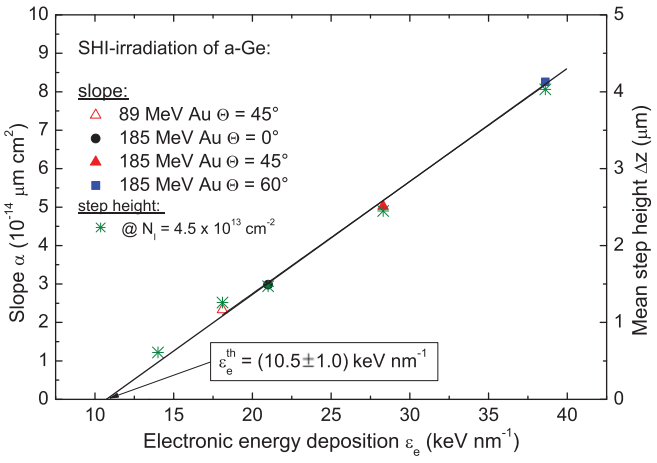

FIG. 6. (Color online) Slope α as well as mean step height Δz for an ion fluence of 4.5×10^{13} cm^{-2} versus the electronic energy deposition ϵ_e for swift heavy-ion irradiation of 3.1 μm-thick amorphous germanium layers.

also confirmed by the five mean step heights obtained after ion irradiation with a fixed ion fluence of 4.5×10^{13} cm^{-2} (cf. Table II) but at different values of ϵ_e, which are also included in Fig. 6 (right-hand scale). In addition, molecular dynamics simulations were done, which show an excellent qualitative agreement with our experimental results, namely, the linear dependence between volume increase and ion fluence and electronic energy deposition as well as the threshold in energy deposition for void formation.[43]

The threshold thus determined enables an explanation of the results achieved in the case of irradiated c-Ge. As mentioned above, the swelling of the crystalline sample is constant over a wide range of ion fluences but increases at high ion fluences (cf. Fig. 2). The reason for this becomes evident in the cross-section SEM image shown in Fig. 7. Compared to the amorphous samples (cf. Figs. 3 and 5), no porous layer can be seen at the surface, which is still crystalline and free of voids, consistent with the fact that no significant changes in reflectivity are observed. However, it is the formation of a *buried* porous layer (bright band) evident in Fig. 7 that causes the increased step height at high ion fluences. A similar buried porous layer next to the porous surface layer was observed for irradiation of a Ge sample with a 3.1 μm-thick amorphous surface layer under the same conditions (185 MeV Au and 45° angle of incidence) (see Ref. 10). In both cases, the buried porous layer is located at a depth of ≈6.5 μm relative to the initial surface. This depth corresponds to approximately two-thirds the depth of the maximum nuclear energy deposition, which becomes evident from the included depth profile of ϵ_n and ϵ_e in Fig. 7. Consequently, the formation of the buried layer cannot be attributed to the atomistic processes by which porosity is generated via nuclear energy deposition for low ion energies,[1–8] because obviously no voids are observed in the depth of the maximum of ϵ_n (≈10 μm).[42] However, the nuclear energy deposition does result in the formation of a buried amorphous layer around the maximum of ϵ_n, which broadens toward the surface with increasing ion fluence. The calculation of ϵ_e at a depth of ≈6.5 μm for the given irradiation conditions using SRIM 2008[42] reveals a value of ≈10.5 keV nm^{-1}, which is a good agreement with the electronic energy deposition threshold of 10.5 ± 1.0 keV nm^{-1} for void formation in a-Ge mentioned above. Thus, a buried porous layer is formed at depths where ϵ_e exceeds the threshold value *and* where the initially crystalline material is amorphized due to nuclear energy deposition. This only occurs after irradiation of a sufficiently high ion fluence, and thus the swelling of c-Ge remains constant over a wide fluence range but then significantly increases above $N_I \approx 1.0 \times 10^{14}$ cm^{-2}.

Thus, the long-standing question concerning the formation depth of buried porous layers during SHI irradiation of c-Ge[9] can now be explained by the threshold value for void formation determined in the present experiment. Like the results of our c-Ge irradiations, the authors of Ref. 9 reported that all buried porous layers were formed at depths where the electronic energy deposition was ≈10 keV nm^{-1}. Based on these results, one may therefore conclude that voids are formed in a-Ge if a threshold value of ≈10 keV nm^{-1} of the energy deposited in electronic processes is exceeded.

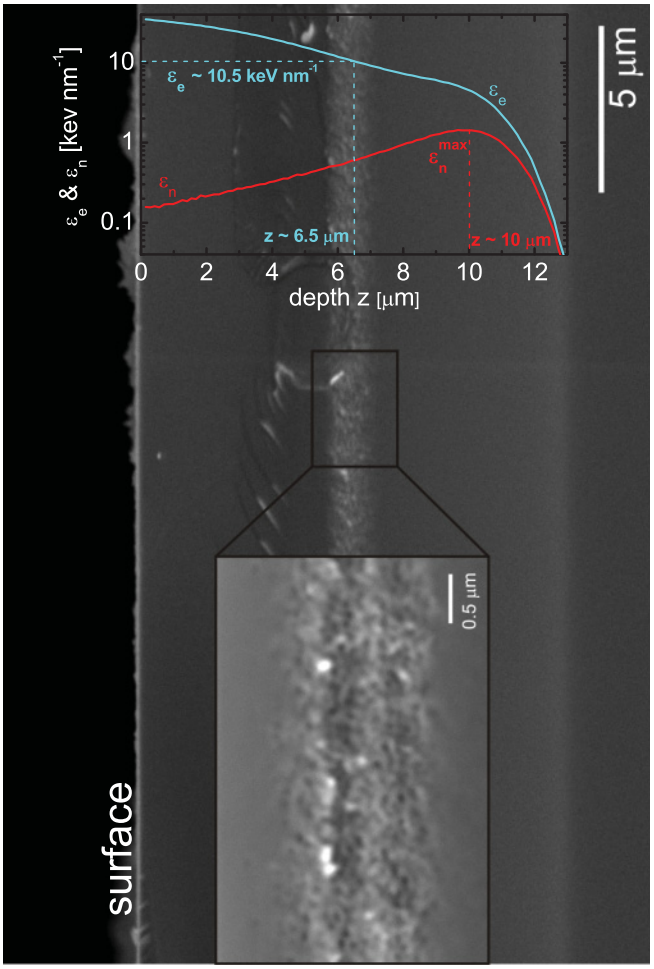

FIG. 7. (Color online) XSEM image (XSEM 1) of a crystalline germanium sample irradiated with 185 MeV Au ions at a 45° angle of incidence ($N_I = 1.5 \times 10^{14}$ cm^{-2}), showing the formation of a buried porous layer at a depth of approximately 6.5 μm. Inset: higher-magnification view of the buried porous layer. In addition, SRIM calculations of electronic ϵ_e (solid blue line) and nuclear ϵ_n (solid red line) energy deposition versus depth z are included for direct comparison (see text).

B. Plastic deformation

The plastic deformation of amorphous layers during SHI irradiation that conserves the macroscopic volume was successfully described by the modified viscoelastic Maxwell model,[27,28,37,44] whereas the most successful approach to explain the underlying ion-solid interaction is the viscoelastic model by Trinkaus and Ryazanov[45] and Trinkaus.[46–49] In this model they extracted a surface shift, which is given by the well-established relation[27,28,34–37,44]

$$\Delta x = 3A_0(\epsilon_e)d_a N_I \sin(2\Theta), \tag{2}$$

where $A_0(\epsilon_e)$ is the deformation yield, which is a function of ϵ_e and d_a is the thickness of the amorphous layer. As mentioned, this model postulates volume conservation during ion irradiation, which is clearly not the case for SHI irradiation of a-Ge at room temperature as shown above. Hence, the present results cannot be fitted linearly (dashed black line in Fig. 4) due to the volume expansion. This inhibits a quantification of the deformation yield A_0 according to Eq. (2). Taking into account the swelling, that is, the volume expansion of the amorphous layer caused by void formation, which is a linear function of the ion fluence [cf. Fig. 2 and Eq. (1)], the following relation is proposed:

$$\Delta x = 3A_0(\epsilon_e)d_a N_I \sin(2\Theta) + B(\alpha)N_I^2. \tag{3}$$

Fits based on Eq. (3) are plotted in Fig. 4 (solid and dashed lines). The agreement with the data points is excellent. Thus, the experimentally observed behavior of Δx is well described by the superposition of a linear term, $\Delta x \propto N_I$, and a quadratic term, $\Delta x \propto N_I^2$ (with a fit parameter B), according to Eq. (3). However, it must be mentioned that in many amorphous solids, plastic deformation indicates the existence of an incubation fluence,[24,28,51] which is in the range of $\approx 10^{12}$ cm^{-2} and roughly corresponds to a complete overlap of the surface with ion tracks. The analysis of our data based on a two-hit model, that is, consideration of an incubation fluence F_{inc}, shows that the derived incubation fluence is very small (of the order of 10^{10} cm^{-2}). Thus, the analysis shows no difference in the values of the fit parameters achieved from our calculations (one-hit model). The even higher fixed incubation fluence of 1.0×10^{12} cm^{-2} does not change the fit parameters significantly, that is, the differences are much smaller than the fit errors. Moreover, investigation of the plastic deformation in a-Si revealed that the shear rate is very low (in the range of 10 nm s^{-1}), and therefore the ion fluences, which are necessary to observe the tiny plastic deformation effect, are high (in the range of 10^{14}–10^{15} cm^{-2}).[34] Consequently, a possible threshold that was expected in the range of $F_{\text{inc}} = 10^{12}$ cm^{-2} (2 orders of magnitude difference) could not be determined.[34] To observe plastic deformation in a-Ge, sufficiently high ion fluences, in the range of 10^{13}–10^{14} cm^{-2} are required as well. Hence, the use of a two-hit model is not necessary because the incubation fluence is negligible.

Thus, provided that both terms act independently, the observed enhanced plastic flow process may be explained by the additional quadratic term, while the linear term may

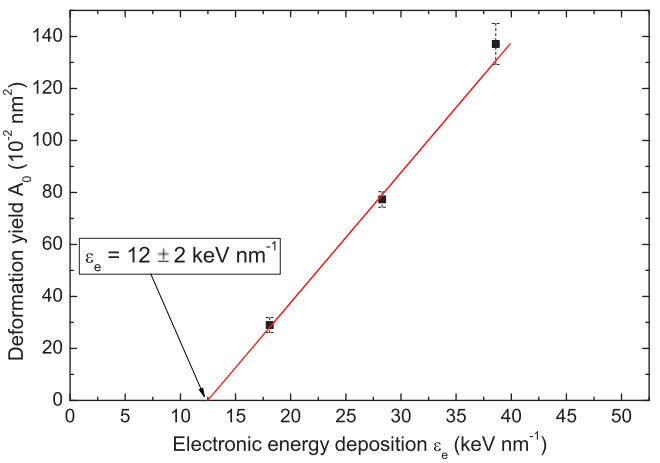

FIG. 8. (Color online) Deformation yield A_0 as a function of the electronic energy deposition ϵ_e, indicating the existence of an electronic energy deposition threshold of $\epsilon_e = 12 \pm 2$ keV nm^{-1}.

be attributed to the (volume-conserving) plastic flow process. This assumption enables a quantification of the deformation yield A_0 by means of the linear term in Eq. (3). The results are plotted in Fig. 8 as a function of the electronic energy deposition ϵ_e. Above a threshold value of $\epsilon_e = 12 \pm 2$ keV nm^{-1}, the deformation yield increases linearly with ϵ_e and a slope of $\partial A_0/\partial \epsilon_e = 5.0 \times 10^{-2}$ nm^3 keV^{-1}.

The energy deposition threshold for the plastic deformation of a-Ge obtained herein is of the same order of magnitude as those previously reported for glasses such as vitreous silica ($\epsilon_e = 2.5$ keV nm^{-1}),[50] metal glass $Fe_{85}B_{15}$ ($\epsilon_e = 13$ keV nm^{-1}),[51,52] and glassy $Pd_{80}Si_{20}$ ($\epsilon_e = 23$ keV nm^{-1})[52] as well as a-Si, where an energy deposition threshold of $\epsilon_e = 14.2$ keV nm^{-1} was determined.[34] Note that, while the analysis made above is not based on any theoretical model, the present experimental results of SHI irradiation of a-Ge nevertheless show all the characteristics of ion hammering like a-Si[34–36] and, therefore, support the recently discussed idea[10,34] that liquid polymorphism is a general phenomenon in tetrahedral networks.

V. CONCLUSION

The influence of high electronic energy deposition on void formation as well as the plastic flow process in SHI-irradiated a-Ge layers was investigated. For all irradiation parameters used, a strong swelling of the irradiated material was observed, which depends linearly on the ion fluence. This volume expansion is caused by the formation and growth of randomly distributed voids, leading to a gradual transformation of the amorphous layer into a sponge-like porous structure as established by XSEM investigations. Moreover, the rate of the volume expansion increases linearly with increasing electronic energy deposition, thus clearly demonstrating that the structural changes are determined solely by the electronic energy deposited within the amorphous layer. An electronic energy deposition threshold for void formation could be determined, yielding $\epsilon_e = 10.5 \pm 1.0$ keV nm^{-1}. SHI irradiation of a-Ge at room temperature and nonperpendicular ion incidence leads to fluence-dependent plastic flow in the direction of the ion beam projection on the surface. We demonstrate that this effect is a nonlinear process, that is, an enhanced plastic flow was observed as a consequence of the extreme void formation within the amorphous layer. By a simple approach, the experimentally observed behaviour of the surface shift was well described, thus providing the derivation of the deformation yield for the different irradiation parameters. It was shown that above a threshold value for the ion hammering effect in a-Ge, which was estimated at $\epsilon_e = 12 \pm 2$ keV nm^{-1}, the deformation yield increases linearly with the electronic energy deposition. Furthermore, based on these results, the longstanding question concerning the reason for structural modification observed in SHI-irradiated c-Ge, where the formation of a buried porous layer was observed, was explained and discussed.

ACKNOWLEDGMENTS

The research was supported by the Bundesministerium für Bildung und Forschung (BMBF; Contract No. 05KK7SJ1) and Deutscher Akademischer Austausch Dienst (DAAD; Contract No. D/07/15034). We would like to thank the staff at the ANU Heavy-Ion Accelerator Facility for technical assistance.

*Corresponding author. tobias.steinbach@uni-jena.de

[1] I. H. Wilson, J. Appl. Phys. **53**, 1698 (1982).
[2] B. R. Appleton, O. W. Holland, J. Narayan, O. E. Schow, J. S. Williams, K. T. Short, and E. Lawson, Appl. Phys. Lett. **41**(8), 711 (1982).
[3] O. W. Holland, B. R. Appleton, and J. Narayan, J. Appl. Phys. **54**(5), 2295 (1983).
[4] B. R. Appleton, O. W. Holland, D. B. Poker, J. Narayan, and D. Fathy, Nucl. Instrum. Methods Phys. Res. B **7/8**, 639 (1985).
[5] L. M. Wang and R. C. Birtcher, Phil. Mag. A **64**(6), 1209 (1991).
[6] B. Stritzker, R. G. Elliman, and J. Zou, Nucl. Instrum. Methods Phys. Res. B **175–177**, 193 (2001).
[7] T. Janssens, C. Huyghebaert, D. Vanhaeren, G. Winderickx, A. Satta, M. Meuris, and W. Vandervorst, J. Vac. Sci. Technol. B **24**(1), 510 (2006).
[8] J. Yanagisawa, K. Takarabe, K. Ogushi, K. Gamo, and Y. Akasaka, J. Phys. Condens. Matter **19**, 445002 (2007).
[9] H. Huber, W. Assmann, R. Grötzschel, H. D. Mieskes, A. Mücklich, H. Nolte, and W. Prusseit, Mater. Sci. Forum **248–249**, 301 (1997).
[10] W. Wesch, C. S. Schnohr, P. Kluth, Z. S. Hussain, L. L. Araujo, R. Giulian, D. J. Sprouster, A. P. Byrne, and M. C. Ridgway, J. Phys. D Appl. Phys. **42**, 115402 (2009).
[11] Based on reanalyses of the ion fluence determination of the irradiation setup, the ion fluences in Ref. 10 have to be corrected by a factor of 0.45 to allow comparison with the results given here.
[12] R. L. Fleischer, P. B. Price, and R. M. Walker, J. Appl. Phys. **36**, 3645 (1965).
[13] R. L. Fleischer, P. B. Price, and R. M. Walker, *Nuclear Tracks in Solids* (University of California Press, Berkeley, 1975).
[14] D. Lesueur and A. Dunlop, Rad. Eff. Def. Solids **126**, 163 (1993).
[15] P. Stampfli and K. H. Bennemann, Phys. Rev. B **49**, 7299 (1994).
[16] P. Stampfli, Nucl. Instrum. Methods Phys. Res. B **107**, 138 (1996).
[17] P. L. Silvestrelli, A. Alavi, M. Parrinello, and D. Frenkel, Phys. Rev. B **56**, 3806 (1997).
[18] A. Cavalleri, K. Sokolowski-Tinten, J. Bialkowski, and M. Schreiner, J. Appl. Phys. **85**, 3301 (1999).
[19] S. K. Sundaram and E. Mazu, Nature Mater. **1**, 217 (2002).
[20] M. Toulemonde, C. Dufour, and E. Paumier, Phys. Rev. B **46**, 14362 (1992).
[21] M. Toulemonde, J. M. Costantini, C. Dufour, A. Meftah, E. Paumier, and F. Studer, Nucl. Instrum. Methods Phys. Res. B **126**, 37 (1996).
[22] M. Toulemonde, C. Dufour, E. Paumier, and F. Pawlak, Mater. Res. Soc. Symp. Proc. **504**, 99 (1999).
[23] S. Klaumünzer and G. Schumacher, Phys. Rev. Lett. **51**, 1987 (1983).
[24] S. Klaumünzer, M. D. Hou, and G. Schumacher, Phys. Rev. Lett. **57**, 850 (1986).
[25] M. D. Hou, S. Klaumünzer, and G. Schumacher, Phys. Rev. B **41**, 1144 (1990).

[26] A. I. Ryazanov, A. E. Volkov, and S. Klaumünzer, Phys. Rev. B **51**, 12107 (1995).
[27] S. Klaumünzer, Multisc. Phenom. Plast. Nato Science Series **367**, 441 (2000).
[28] S. Klaumünzer, Nucl. Instrum. Methods Phys. Res. B **225**, 136 (2004).
[29] W. Wesch, A. Kamarou, and E. Wendler, Nucl. Instrum. Methods Phys. Res. B **225**, 111 (2004).
[30] A. Kamarou, W. Wesch, E. Wendler, A. Undisz, and M. Rettenmayr, Phys. Rev. B **73**, 184107 (2006).
[31] C. S. Schnohr, P. Kluth, R. Giulian, D. J. Llewellyn, A. P. Byrne, D. J. Cookson, and M. C. Ridgway, Phys. Rev. B **81**, 075201 (2010).
[32] W. Wesch, A. Kamarou, E. Wendler, A. Undisz, and M. Rettenmayr, Nucl. Instrum. Methods Phys. Res. B **257**, 283 (2007).
[33] W. Wesch, A. Kamarou, and E. Wendler, Nucl. Instrum. Methods Phys. Res. B **225**, 111 (2004).
[34] A. Hedler, S. Klaumünzer, and W. Wesch, Nature Mater. **3**, 804 (2004).
[35] A. Hedler, S. Klaumünzer, and W. Wesch, Phys. Rev. B **72**, 054108 (2005).
[36] A. Hedler, S. Klaumünzer, and W. Wesch, Nucl. Instrum. Methods Phys. Res. B **242**, 85 (2006).
[37] A. Gutzmann and S. Klaumünzer, Nucl. Instrum. Methods Phys. Res. B **127/128**, 12 (1997).
[38] T. Som, J. HGhatak, O. Sinha, R. Sivakumar, and D. Kanjilal, J. Appl. Phys. **103**, 123532 (2008).
[39] S. Furuno, H. Otsu, K. Hojou, and K. Izui, Nucl. Instrum. Methods Phys. Res. B **107**, 223 (1996).
[40] A. Kamarou, E. Wendler, A. Undisz, M. Rettenmayr, and W. Wesch, Phys. Rev. B **78**, 054111 (2008).
[41] J. Costantini, F. Brisard, M. Toulemonde, and F. Studer, Nucl. Instrum. Methods Phys. Res. B **122**, 514 (1997).
[42] J. F. Ziegler, J. P. Biersack, and U. Littmark, *The Stopping and Range of Ions in Solids* (Pergamon, Oxford, 2003).
[43] K. Gärtner, T. Steinbach, J. Jöhrens, C. S. Schnohr, M. C. Ridgway and W. Wesch, in preparation.
[44] A. Gutzmann, S. Klaumünzer, and P. Meier, Phys. Rev. Lett. **74**, 2256 (1995).
[45] H. Trinkaus and A. I. Ryazanov, Phys. Rev. Lett. **74**, 5072 (1995).
[46] H. Trinkaus, J. Nucl. Mater. **223**, 196 (1995).
[47] H. Trinkaus, Nucl. Instrum. Methods Phys. Res. B **107**, 155 (1996).
[48] H. Trinkaus, J. Nucl. Mater. **246**, 244 (1997).
[49] H. Trinkaus, Nucl. Instrum. Methods Phys. Res. B **146**, 204 (1998).
[50] S. Klaumünzer, Mater. Sci. Forum **97–99**, 623 (1992).
[51] A. Audouard, B. Balanzat, G. Fuchs, J. C. Jousset, D. Lesueur, and L. Thomé, Europhys. Lett. **3**, 327 (1987).
[52] A. Audouard, B. Balanzat, J. C. Jousset, D. Lesueur, and L. Thomé, J. Phys. Condens. Matter. **5**, 995 (1993).